RSC Advances

PAPER

View Article Online
View Journal | View Issue

Cite this: *RSC Adv.*, 2017, **7**, 22256

An ionic liquid doped electrochemical copolymer coating of indole and 3-methylthiophene for the solid-phase microextraction of polycyclic aromatic hydrocarbons†

Xiafei Guo, Aiziguli mulati, Mian Wu, Jie Zhang, Liu Yang, Faqiong Zhao and Baizhao Zeng *

A novel poly(indole-*co*-3-methylthiophene)–ionic liquid (*i.e.*, 1-allyl-3-vinylimidazolium bis((trifluoromethyl)sulfonyl)imide) (P(In–3-MeT)/IL) composite film was electrodeposited on a stainless steel wire for headspace solid phase microextraction. The obtained P(In–3-MeT)/IL coating was rough and showed a cauliflower-shape. It had high thermal stability (up to 450 °C) and mechanical stability and could be used for at least 180 times in solid phase microextraction (SPME) without a decrease in extraction performance. The coating exhibited high extraction capacity for some polycyclic aromatic hydrocarbons (*e.g.* naphthalene, 1-methylnaphthalene, acenaphthene, biphenyl, fluorene and phenanthrene) due to the strong hydrophobic and π–π interactions between the analytes and P(In–3-MeT)/IL. Through coupling with GC, good linearity (correlation coefficients higher than 0.9994), wide linear ranges (0.05–50 μg L^{-1}) and low limits of detection (6.25–25.2 ng L^{-1}) were achieved for these analytes. The reproducibility (defined as RSD) was 3.5–5.5% and 4.5–7.2% for single fiber ($n = 5$) and fiber-to-fiber ($n = 5$), respectively. The SPME-GC method was successfully applied for the determination of three real samples, and the recoveries for standards added were 86.8–105% for mosquito-repellent incense, 89.9–110% for cigarettes and 82.3–103% for industrial lubricant.

Received 25th February 2017
Accepted 7th April 2017

DOI: 10.1039/c7ra02372c

rsc.li/rsc-advances

1. Introduction

Solid-phase microextraction (SPME), which was first introduced by Pawliszyn and coworkers in the 1990s, is a useful sample-pretreatment technique.[1] It is able to integrate sampling, isolation, trace enrichment, clean-up process and sample introduction into one step.[2] With the merits of lack of organic solvent, simple operation, easy automation and coupling with gas chromatography (GC),[3] gas chromatography-mass spectrometry (GC-MS),[4] high performance liquid chromatography (HPLC),[5] capillary electrophoresis (CE),[6] *etc.*, it has been widely applied for the analysis of food,[7] clinical,[8] environmental[9] and biological[10] samples. The key part of SPME is the coating. Therefore, the development of the coating is of great importance to achieve high extraction efficiency and selectivity.

Among various fabricating methods, electropolymerization is a favorable method to deposit conductive polymer films directly on solid surface. This method was attempted by Wu and Pawliszyn *et al.* a decade ago, and polypyrrole and polyaniline (PANI) SPME coatings were constructed.[11,12] Since the pioneering work on the aniline based copolymers was reported by Wei *et al.*, copolymerization of aromatic monomers (*e.g.*, biphenyl, thiophene, pyrrole), either under potentiostatic or using dynamic conditions, has been widely applied.[13,14] By combining different monomers, it is possible to synthesize copolymers with high stability and high extraction efficiency. Xu *et al.*[15] fabricated a poly(*p*-phenylenediamine-*co*-aniline) composite coating on a stainless steel wire (SSW) for the head-space SPME of some derivatives of benzene; it displayed improved porous structure and higher extraction efficiency than the PANI coating. Ai *et al.*[16] prepared a hydrophobic coating of polyaniline–poly(propylene oxide) copolymer for direct immersion solid phase microextraction of carbamate pesticides; it showed strong hydrophobicity, good anti-fouling ability and repeatability. Kazemipour *et al.*[17] reported a nanocomposite sorbent concerning poly(*o*-phenylenediamine-*co*-*o*-toluidine) modified carbon nanotubes for the detection of polycyclic aromatic hydrocarbons by coupling with GC; it showed favourable extraction capability and long lifetime. Recently, poly(3-methylthiophene) (P3MeT) and polyindole (PIn), as conducting polymers with p-conjugated electronic structures, have received significant attention. P3MeT has high conductivity and

Key Laboratory of Analytical Chemistry for Biology and Medicine (Ministry of Education), College of Chemistry and Molecular Science, Wuhan University, Wuhan, Hubei 430072, PR China. E-mail: bzzeng@whu.edu.cn; Fax: +86-27-68754067; Tel: +86-27-68752701

† Electronic supplementary information (ESI) available. See DOI: 10.1039/c7ra02372c

flexibility, but its thermal property is relatively poor in contrast to PIn film.[18] When coupled with GC, P3MeT might be destroyed by high temperature. PIn owns fairly good thermal stability because of the incorporation of benzene rings on the polymer backbone and high mechanic stability. However, PIn has relatively low electrical conductivity.[18] The electrodeposited PIn film generally is non-uniform and thin. By electrochemical copolymerization of indole and 3-methylthiophene, their merits might be combined and a good coating might be obtained.

Ionic liquids (ILs), composed of organic cations and organic or inorganic anions, are a class of non-molecular solvents. They display favorable physicochemical characteristics such as non-volatility, good electrical conductivity, wide electrochemical window, high thermal stability,[19,20] which make them possess good application potential in electropolymerization. The application of IL as dopant in electropolymerization can improve the structure of polymers. Zhao *et al.*[21] fabricated a PANI–IL composite film on platinum wire for the detection of benzene derivatives, and it showed porous structure and excellent adsorption capacity. Besides, it has been reported that the performance, lifetime and stability of conducting polymers could be improved by using IL electrolytes.[22–24] Therefore, IL is considered as stationary phase for SPME. Cagliero *et al.*[25] reported a matrix-compatible sorbent coating based on structure-tuned polymeric ionic liquid, and it was used to determinate acrylamide in brewed coffee and coffee powder. Wu *et al.*[26] prepared a metal–organic framework–IL functionalized graphene nanocomposite by *in situ* solvothermal growth, which was used for highly efficient enrichment of chloramphenicol and thiamphenicol. Feng *et al.*[27] fabricated a MWCNTs doped-PIL fiber by *in situ* polymerization with stainless steel wire as support, and it was applied for the SPME of 2-naphthol in aqueous and citrus samples.

In this work, a novel poly(indole-*co*-3-methylthiophene)/IL (P(In–3-MeT)/IL) composite coating was prepared by electrochemical method in acetonitrile (ACN) solution containing 1-allyl-3-vinylimidazolium bis((trifluoromethyl)sulfonyl)imide ([AVIm]NTf_2). The coating was smooth and the thickness was uniform. It combined the advantages of PIn, P3MeT and IL and demonstrated high selectivity toward PAHs due to the strong hydrophobic and π–π interaction. When it was used for the determination of PAHs by coupling with GC, it presented good thermal, chemical and mechanical stability, low limits of detection (LODs) and high sensitivity.

2. Experimental

2.1 Apparatus

A CHI 617A electrochemical workstation (CH Instrument Corp., Shanghai, China) was employed for preparing SPME fibers. A conventional three-electrode system was adopted, including a stainless steel wire (2 cm × 250 μm O.D.) as working electrode, a Pt wire (2.5 cm × 0.1 cm O.D.) as counter electrode and an Ag/AgCl electrode as reference electrode. The SPME device was laboratory-made, and it was a modified 5 μL syringe. Commercial SPME fibers (100 μm polydimethylsiloxane (PDMS)) was supplied by Supelco (Bellefonte, PA, USA). The scanning electron microscopy (SEM) images were obtained by using an LEO 1530 field emission SEM (Carl Zeiss NTS GmbH, Germany).

A SP-6890 GC equipped with a flame ionization detector (FID) (Shandong Lunan Ruihong Chemical Instrument, Tengzhou, China) and a N2000 chromatographic workstation (Zhenjiang University, Zhejiang, China) were used in this work. The analysis of PAHs was performed on a SE-54 capillary column (5% phenyl–95% methyl polysilicone, 30 m × 320 μm × 0.33 μm, Lanzhou Atech Technologies, Lanzhou, China). The following column temperature program was used: 50 °C held for 4 min, followed by increasing temperature to 200 °C at a rate of 19 °C min^{-1}, then at a rate of 4.5 °C min^{-1} to 240 °C, which was held for 2 min; finally it was programmed at 2 °C min^{-1} to 250 °C, which was held for 2 min. The total run time was 30 min. The inlet was operated under splitless mode; the injector port temperature and detector temperature were set at 250 °C. Ultrapure nitrogen was used as carrier gas at 1 mL min^{-1} and makeup gas at 30 mL min^{-1}, respectively.

2.2 Reagents and materials

All chemicals and reagents were of analytical grade. 1-Butyl-1-methylpiperidinium bis[(trifluoromethyl)sulfonyl]imide ([PP_{14}]NTf_2), 1-hydroxyethyl-3-methylimidazolium bis[(trifluoromethyl)sulfonyl]imide ([HOEMIm]NTf_2) and 1-allyl-3-vinylimidazolium bis((trifluoromethyl)sulfonyl)imide ([AVIm]NTf_2) were purchased from Lanzhou institute of Chemical Physics (Gansu, China). 3-MeT and tetrabutylammonium perchlorate (TBAP) were purchased from Aladdin Chemistry Co., Ltd. (Shanghai, China). Indole, NaCl, naphthalene (NAP), 1-methylnaphthalene (1-MNAP), biphenyl (BP), acenaphthene (ACE), fluorene (FLU), phenanthrene (PHE), septas and vials came from the Reagent Factory of Shanghai. The stock solution of PAHs (0.010 mg mL^{-1} for all analytes) was prepared with absolute methanol and stored at −4 °C. The samples, including mosquito-repellent incense, cigarette and industrial lubricant, were purchased from the local supermarket (Wuhan, China). The mosquito-repellent incense sample was crushed by mortar before use. The cigarette sample was pretreated by liquid extraction with methanol[28] prior to SPME procedure. Briefly, the cigarette (5.0 g) was added to a glass bottle, then 50 mL methanol was added. The bottle was capped and shaken for 24 h. After that, the extractant was collected for SPME.

2.3 Preparation of P(In–3-MeT)/IL coating

The polymer film was directly electrodeposited on stainless steel wire surface in ACN solution containing 0.10 M TBAP, 0.020 M In, 0.20 M 3-MeT and 0.2% (v/v, *i.e.*, 20 μL per 10 mL) [AVIm]NTf_2 by using cyclic voltammetry (CV) technique. Prior to electrochemical deposition, the stainless steel wire was rinsed thoroughly with methanol and deionized water, and then was dried with infrared lamp. The CV was operated at a scan rate of 50 mV s^{-1} between −0.2 and 1.6 V and the number of scan cycle was set at 40. During the electrochemical polymerization, the surface of the stainless steel wire gradually became black, indicating the formation of P(In–3-MeT)/IL film (Fig. 1). The obtained fiber was washed with

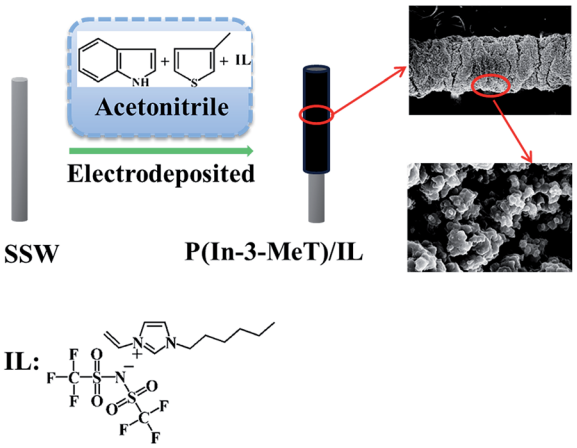

Fig. 1 Schematic formation process of P(In–3-MeT)/IL coating.

distilled water to remove unwanted chemicals such as monomer and supporting electrolyte, and subsequently was kept in a desiccator for 24 h at room temperature. Afterwards, it was aged in a muffle furnace at 100 °C for 30 min and then 280 °C for 2 h under a gentle stream of N_2. Finally, the fiber was installed into the laboratory-made SPME device. For comparing study, P(3-MeT), PIn and P(In–3-MeT) coatings were also electrodeposited on the stainless steel wire surface under the same conditions but without IL.

2.4 SPME procedure

A 10 mL aqueous solution was transferred into a 15 mL glass vial with PTFE septum. After adding 3.5 g NaCl, a magnetic stirring bar and 5 μg L^{-1} PAHs, the vial was tightly sealed with an aluminum cap to prevent sample loss, and then was put in a water bath. The magnetic stirrer was used to accelerate the extraction. When the temperature reached the fixed value, the fiber was exposed to the headspace over the stirred solution for fixed time. Then the fiber was withdrawn into the needle, removed from the sample vial and immediately introduced into the GC injector port for thermal desorption of 4 min. Each measurement was carried out in triplicate. The same procedure was adopted for the determination of samples. When the recoveries for the standards added were tested, 5.0 μL 5.0 μg L^{-1} PAHs solution was spiked in mosquito-repellent incense sample, cigarette sample and industrial lubricant extraction.

3. Results and discussion

3.1 Optimization of the ratio of In and 3-MeT

The ratio of In and 3-MeT could affect the resulting coating structure, in order to achieve high extraction efficiency their concentration ratio (M/M) was changed (*i.e.* 2 : 1, 1 : 1, 1 : 5, 1 : 10 and 1 : 20). As a result, when it was 2 : 1 and 1 : 1, the obtained coating was not uniform and the stainless steel wire could not be well covered. When it decreased to 1 : 5, 1 : 10 and 1 : 20, the coating became well-defined and smooth. The extraction efficiency of different coatings was compared in Fig. 2. When the ratio was 1 : 10, higher extraction efficiency was achieved.

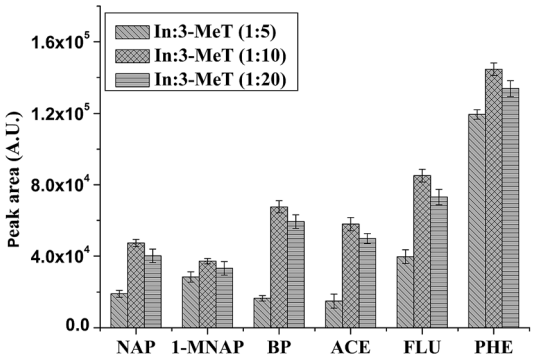

Fig. 2 Influence of the ratio of In and 3-MeT on extraction efficiency of resulting P(In–3-MeT)/IL fiber for the PAHs. Concentration of PAHs: 5 μg L^{-1}; extraction temperature: 20 °C; NaCl concentration: 0.35 g mL^{-1}; stirring rate: 500 rpm; extraction time: 40 min; desorption time: 4 min; desorption temperature: 250 °C. Error bars show the standard deviation ($n = 3$).

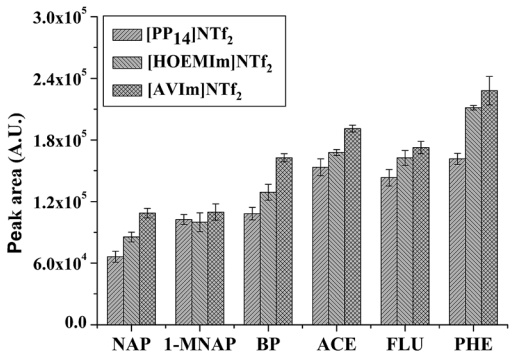

Fig. 3 Effect of IL (*i.e.*, [AVIm]NTf_2, [HOEMIm]NTf_2 and [PP_{14}]NTf_2) on the GC peak area of the PAHs after HS-SPME. Other conditions are the same as in Fig. 2. Error bars show the standard deviation ($n = 3$).

3.2 Optimization of IL

3.2.1 Selection of IL. Considering the PAHs possessing rich stacking π electrons and easily causing π–π interaction, several ILs containing different stacking π electrons (*i.e.*, [AVIm]NTf_2, [HOEMIm]NTf_2 and [PP_{14}]NTf_2) were used for the preparation of P(In–3-MeT)/IL coating under the same conditions. Their coating thickness was kept almost the same. As shown in Fig. 3, the resulting P(In–3-MeT)/ILs coatings display different extraction efficiency due to the change of cations, and the P(In–3-MeT)/[AVIm]NTf_2 demonstrates higher extraction efficiency than the other two. The possible reason is that: the [AVIm]NTf_2 possesses richer stacking π electrons than the other two, easily causing strong π–π interaction.

3.2.2 Optimization of the volume of [AVIm]NTf_2. The volume of [AVIm]NTf_2 was varied from 10 μL to 30 μL to test its effect. Results indicated that the extraction efficiency increased as the volume was enhanced (Fig. 4). However, when the volume exceeded 20 μL (the total volume of the solution was 10 mL), the extraction efficiency decreased. The reason might be that excess IL hindered the electropolymerization of In–3-MeT to some extent. Hence, 20 μL was adopted as the optimized volume.

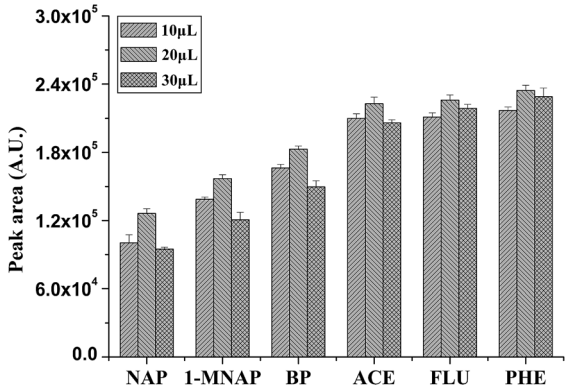

Fig. 4 Influence of the volume of [AVIm]NTf_2 on extraction efficiency of P(In–3-MeT)/IL fiber for the PAHs. Volume of [AVIm]NTf_2: 10 μL, 20 μL, 30 μL; the total volume of electrolyte solution: 10 mL. Other conditions are the same as in Fig. 2. Error bars show the standard deviation ($n = 3$).

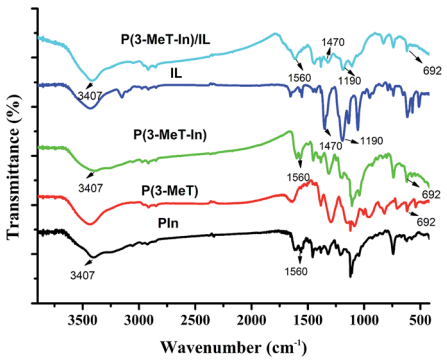

Fig. 5 FTIR spectra of P(In–3-MeT)/IL, IL, P(In–3-MeT), P(3-MeT) and PIn.

3.3 Characterization of P(In–3-MeT)/IL composite coating

3.3.1 FTIR spectra. The FT-IR spectra of P(In–3-MeT)/IL, IL, P(In–3-MeT), P(3-MeT) and PIn were shown in Fig. 5. In the case of P(In–3-MeT), the strong and broad peaks at 3407 cm^{-1} and 1560 cm^{-1} were the characteristic peak of PIn, the strong and broad peak at 3407 cm^{-1} was the characteristic absorption of the N–H bond, and the band together with the band at 1560 cm^{-1} could be ascribed to the elongation and the deformation vibrations of the N–H bond, respectively.[18] The peak at 692 cm^{-1} was the characteristic peak of P(3-MeT), denoting the C–S stretching in the thiophene ring.[29] The FT-IR spectrum of P(In–3-MeT)/IL showed the characteristic vibration bands corresponding to the imidazolium cation. The peak at 1470 cm^{-1} could be ascribed to the stretching vibrations of the C–N bonds in the aromatic system of imidazole and the peak at 1190 cm^{-1} was ascribed to imidazole ring in-plane asymmetric stretching vibration.[30] These absorption bands were accordant with those of IL, indicating that IL was successfully introduced into P(In–3-MeT). These indicated that a composite coating formed.

3.3.2 Thermal stability. The thermal stability of P(In–3-MeT)/IL, P(In–3-MeT), P(3-MeT) and PIn were investigated. As shown in Fig. S1,† PIn started to lose weight when the temperature was over 375 °C. The TGA curve of P(3-MeT) had two evident decomposition processes occurred at 265 and 350 °C, respectively. For the P(In–3-MeT) coating there was an obvious degradation at about 350 °C. Moreover, the P(In–3-MeT)/IL coating showed higher decomposition temperature (>450 °C), meaning that the P(In–3-MeT)/IL coating had good thermal stability.

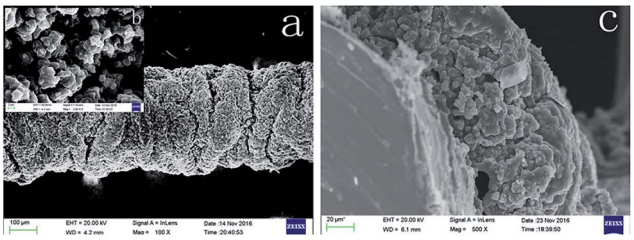

Fig. 6 SEM images of the P(In–3-MeT)/[AVIm]NTf_2 film (a), the cross-section image of P(In–3-MeT)/[AVIm]NTf_2 film (c). Inset: magnified image of P(In–3-MeT)/[AVIm]NTf_2 (b).

3.3.3 Morphology. Fig. 6 shows the SEM image of P(In–3-MeT)/[AVIm]NTf_2 coating. It presents cauliflower-shape structure, and the coating is uniform, with a thickness of about 40 μm. The P(In–3-MeT) coating (Fig. S2a†) presents nodular accumulating structure, and the P(3-MeT) (Fig. S2b†) coating likes aggregated blossoms, the PIn (Fig. S2c†) coating shows dendritic morphology. Therefore, it can be thought that the copolymerization of In and 3-MeT occurred and IL was doped in the copolymer.

3.3.4 Extraction selectivity. Five series of organic compounds, including amines (*i.e.* aniline, *N*-methylacetamide, 3-methylbenzenamine, 2-chlorobenzenamine, 3-chlorobenzena-

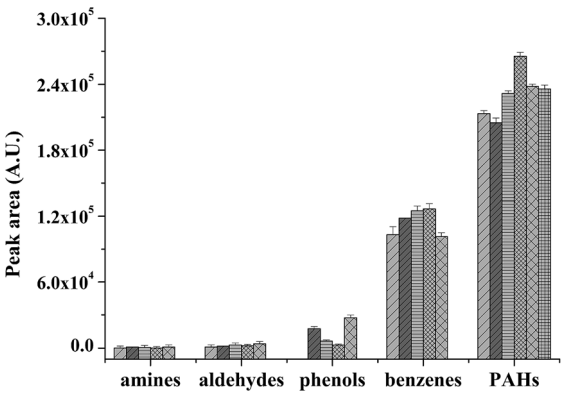

Fig. 7 Extraction efficiency of P(In–3-MeT)/IL fiber for different compounds. Compounds (from left to right): amines (*i.e.* aniline, *N*-methylacetamide, 3-methylbenzenamine, 2-chlorobenzenamine, 3-chlorobenzenamine); aldehydes (*i.e.* salicyl aldehyde, nonyl aldehyde, decyl aldehyde, cinnamal dehyde, citral); phenols (*i.e.* *O*-cresol, *M*-cresol, 4-chlorophenol, 2,6-dichlorophenol); benzenes (*i.e.* bromobenzene, 4-bromotoluene, 3-nitrotoluene, 4-nitrotoluene, 1,2,4-trichlorobenzene); PAHs (*i.e.* naphthalene, 1-methylnaphthalene, biphenyl, acenaphthene, fluorene, phenanthrene). Concentration of PAHs: 5 μg L^{-1}; extraction temperature: 20 °C; NaCl concentration: 0.35 g mL^{-1}; stirring rate: 500 rpm; extraction time: 40 min; desorption time: 4 min; desorption temperature: 250 °C. Error bars show the standard deviation ($n = 3$).

Table 1 Analytical parameters for PAHs measured with P(In–3-MeT)/IL fiber based HS-SPME-GC method

Analytes	LOD (ng L^{-1})	Linear range (μg L^{-1})	Regression equation	Correlation coefficient	RSD (%) One fiber ($n = 5$)	RSD (%) Fiber to fiber ($n = 5$)
NAP	25.2	0.05–50	$Y = 29\,635X + 2062$[a]	0.9979	4.8	5.6
1-MNAP	25.2	0.05–50	$Y = 36\,643X + 20\,651$	0.9994	3.9	6.8
BP	12.5	0.05–50	$Y = 36\,538X + 17\,273$	0.9967	4.2	7.2
ACE	6.25	0.05–50	$Y = 46\,769X + 10\,928$	0.9957	5.1	5.5
FLU	12.5	0.05–50	$Y = 36\,089X + 44\,126$	0.9985	5.5	4.5
PHE	12.5	0.05–50	$Y = 36\,653X + 31\,538$	0.9987	4.2	4.6

[a] Y: peak area; X: concentration (μg L^{-1}).

Table 2 Comparison of analytical data of the proposed method with other reported methods

Methods	Linear ranges (μg L^{-1})	LOD (μg L^{-1})	RSD (%)	Ref.
PEDOT/GO[a]–GC–FID	0.4–600	0.050–0.13	9.8–13	32
PIL–GC–FID	0.5–20	0.050–0.25	9.2–29	33
PILs–GO[a]–GC–FID	0.05–50	0.015–0.025	3.8–11	34
P(In–3-MeT)/IL–GC–FID	0.05–50	0.0062–0.025	3.9–5.5	This work

[a] GO, graphene oxide.

mine), aldehydes (*i.e.* salicyl aldehyde, nonyl aldehyde, decyl aldehyde, cinnamal dehyde, citral), phenols (*i.e. O*-cresol, *M*-cresol, 4-chlorophenol, 2,6-dichlorophenol), benzenes (*i.e.* bromobenzene, 4-bromotoluene, 3-nitrotoluene, 4-nitrotoluene, 1,2,4-trichlorobenzene) and PAHs (*i.e.* naphthalene, 1-methylnaphthalene, biphenyl, acenaphthene, fluorene, phenanthrene) were tested to evaluate the extraction selectivity of the P(In–3-MeT)/IL coating. As could be seen in Fig. 7, the P(In–3-MeT)/IL coating was obviously beneficial to the extraction of PAHs, while it presented low extraction capacity to other compounds tested. This should be ascribed to the strong π–π interaction between the PAHs and the coating besides hydrophobic effect, because [AVIm]NTf_2 and the PAHs both possessed rich stacking π electrons.

3.4 Optimization of extraction conditions

Temperature is a major parameter affecting extraction efficiency, and it was examined from 10 °C to 50 °C. As shown in Fig. S3a,† higher extraction efficiency was observed around 20 °C for the PAHs. Increasing temperature can enhance mass transfer rate of analytes. However, the distribution coefficient of analyte decreases at higher temperature, because surface adsorption is generally an exothermic process. Here low temperature is favorable for the SPME, probably due to the exothermic effect. Hence, 20 °C was adopted for subsequent experiments.

SPME is an equilibrium-based technique and there is a direct relationship between the extracted amount and the extraction time. Extraction time also affects the sensitivity and reproducibility of the raised method. The equilibrium time is generally selected as extraction time. Here, results indicated that the extraction efficiency reached the maximum around 40 min and then it decreased a little (Fig. S3b†). Hence, 40 min was adopted as the optimized extraction time.

The influence of stirring rate on extraction efficiency was also investigated. The solution agitation can promote extraction process and reduce extraction time because the equilibrium can be achieved more rapidly. The stirring speed was varied from 200 to 600 rpm to test its influence in this case. As shown in Fig. S3c,† the extraction efficiency increased with stirring rate changing from 200 to 500 rpm. However, when it was above 500 rpm the rotating of magnetic stirring bar was not very balanced, leading to the decrease of extraction efficiency. Therefore, stirring rate was fixed at 500 rpm in the experiments.

The rise of ionic strength usually causes an increase in the extraction efficiency. This is due to the salting-out effect. In this work, the influence of ionic strength was investigated by varying NaCl concentration from 0.15 to 0.35 g mL^{-1}. As could be seen in Fig. S3d,† the peak area increased when NaCl concentration increased. Thus 0.35 g mL^{-1} NaCl (*i.e.*, saturated NaCl solution) was selected in the experiments.

To examine the release of the extracted analytes in the GC injector port, desorption time was changed from 1 min to 5 min. Result revealed that the peak areas for the six PAHs increased with increasing desorption time up to 4 min at 250 °C, then they kept almost constant (Fig. S3e†). Therefore, 4 min was sufficient for the analytes to desorb from the P(In–3-MeT)/IL fiber at this temperature.

3.5 Method evaluation

Analytical parameters of merit of this P(In–3-MeT)/IL coating were determined and listed in Table 1. The linear ranges were 0.05–50 μg L^{-1}, with correlation coefficients of 0.9957–0.9994.

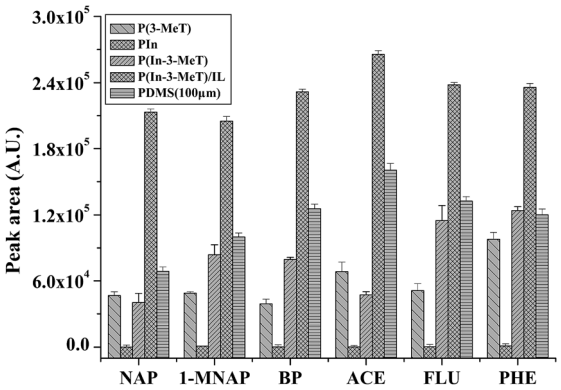

Fig. 8 Comparison of the extraction efficiency of the P(In–3-MeT)/IL fiber, P(In–3-MeT) fiber, P(3-MeT) fiber and PIn fiber and the commercial PDMS (thickness: 100 μm) fiber for the PAHs. The thickness of other coatings: about 40 mm. Other conditions are the same as in Fig. 7. Error bars show the standard deviation ($n = 3$).

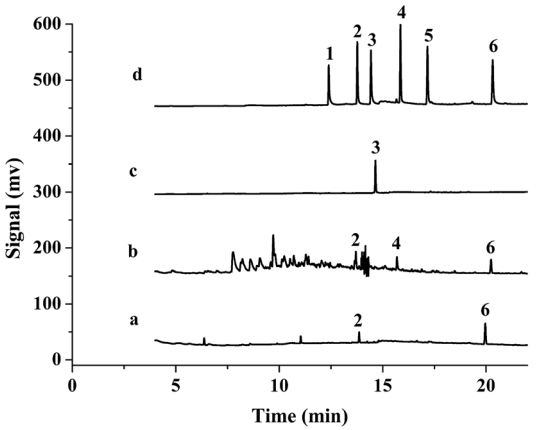

Fig. 9 Typical chromatograms of cigarette extractant (a), industrial lubricant (b), mosquito-repellent incense (c) and 5 μg L^{-1} standard solution (d) after extracted with the P(In–3-MeT)/IL coating, followed by GC-FID analysis. Other conditions are the same as in Fig. 7.

The detection limits (LODs) of the PAHs were estimated to be 6.25–25.2 ng L^{-1}, based on a signal-noise ratio of 3 (S/N = 3).[31] The relative standard deviations (RSDs) for the intra-fiber were 3.9–5.5% ($n = 5$), while for the inter-fiber (four fibers, 3 replicates each) the RSDs were <7.2% for 5 μg L^{-1} PAHs. As could be seen in Table 2, this method was quite good in comparison with other methods in terms of linear range, LOD and repeatability. In addition, the P(In–3-MeT)/IL fiber showed high durability (Fig. S4†). After it underwent 180 adsorption/desorption cycles, its extraction efficiency was almost unchanged. This was related to the high stability and mechanical strength of P(In–3-MeT)/IL coating.

3.6 Extraction capability

The extraction capability of the P(In–3-MeT)/IL fiber, P(In–3-MeT) fiber, P(3-MeT) fiber, PIn fiber and the commercial PDMS (thickness: 100 μm) fiber was compared under the same conditions (Fig. 8). As could be seen, the P(3-MeT) fiber and PIn showed low extraction efficiency for the PAHs, while the P(In–3-MeT) fiber had higher extraction efficiency. However, the extraction efficiency of the P(In–3-MeT)/IL fiber was even higher, although they were prepared by similar method and had same coating thickness. This should be ascribed to the strong π–π interaction between the PAHs and the coating. The extraction efficiency of the P(In–3-MeT)/IL fiber was also higher than that of the commercial PDMS fiber. It indicated that the coating had high extraction capability.

3.7 Application

The proposed method was applied to analyze three samples. A 2 mL cigarette extractant was added into a 8 mL saturated NaCl aqueous solution, and industrial lubricant (0.25 g) and mosquito-repellent incense (0.002 g) were added into a 10 mL saturated NaCl aqueous solution, then they were detected under the optimized conditions. 1-MNAP and PHE were detected in the cigarette extractant and their concentrations were 5.5 and 17.0 μg L^{-1}, respectively. According to the obtained results their contents were calculated to be 0.056 and 0.17 μg g^{-1}, respectively. 1-MNAP, ACE and PHE were detected in the industrial lubricants sample, their concentrations were 1.1, 1.5 and 0.9 μg L^{-1} and their contents were *ca.* 0.044, 0.059 and 0.036 μg g^{-1}, respectively. BP was detected in the mosquito-repellent sample and its concentration was 4.7 μg L^{-1} and the content was calculated to be 23.4 μg g^{-1}. Fig. 9 presents the GC

Table 3 Determination results of PAHs in samples after HS-SPME with. P(In–3-MeT)/IL fiber

	Samples			Recovery[a] (%)		
Analytes	Cigarette (μg L^{-1})	Industrial lubricant (μg L^{-1})	Mosquito-repellent incense (μg L^{-1})	Cigarette	Industrial lubricant	Mosquito-repellent incense
NAP	nd[c]	nd	nd	108 ± 2.3[b]	103 ± 2.5	89.8 ± 3.5
1-MNAP	5.5 ± 0.4[b]	1.1 ± 0.2	nd	92.6 ± 9.8	102 ± 1.6	96.9 ± 5.0
BP	nd	nd	4.7 ± 0.7	110 ± 8.1	95.8 ± 2.5	105 ± 6.8
ACE	nd	1.5 ± 0.5	nd	98.7 ± 6.4	82.3 ± 7.8	99.5 ± 6.6
FLU	nd	nd	nd	89.9 ± 5.1	100 ± 3.8	86.8 ± 5.6
PHE	17.0 ± 0.9	0.9 ± 0.4	nd	92.9 ± 7.1	85.8 ± 3.9	93.2 ± 9.1

[a] Recovery for spiked PAHs solutions. Spiked level: 5 μg L^{-1}. [b] Mean values ± standard deviations. [c] Not detected.

chromatograms of PAHs extracted with the P(In–3-MeT)/IL fiber from the standard solution (d) and the samples (a–c). After spiking in these samples at 5 μg L^{-1}, the recoveries were measured and they were 82.3–110% (Table 3).

4. Conclusions

In this work, we prepared a P(In–3-MeT)/IL composite coating by electrochemical deposition in ACN solution containing [AVIm]NTf_2. Owing to the strong hydrophobic and π–π interaction, the obtained coating exhibited high extraction efficiency and good selectivity for the PAHs. Besides, the P(In–3-MeT)/IL coating displayed high thermal stability, good durable property (could be used for more than 180 times) and reproducibility. Coupled with GC analysis, the P(In–3-MeT)/IL based fiber was used for the determination of several PAHs and it showed wide linear ranges and low detection limits. In addition, it had advantages of easy preparation and low cost. So, the P(In–3-MeT)/IL based fiber had potential application as an useful extraction tool.

Acknowledgements

The authors appreciate the support of the National Natural Science Foundation of China (Grant No. 21275112).

Notes and references

1 C. L. Arthur and J. Pawliszyn, *Anal. Chem.*, 1990, **62**, 2145–2148.
2 C. L. Arthur, L. M. Killam, K. D. Buchholz, J. Pawliszyn and J. R. Berg, *Anal. Chem.*, 1992, **64**, 1960–1966.
3 G. F. Ouyang, D. Vuckovic and J. Pawliszyn, *Chem. Rev.*, 2011, **111**, 2784–2814.
4 C. G. Zambonin and F. Palmisano, *J. Chromatogr. A*, 2000, **874**, 247–255.
5 H. Daimon and J. Pawliszyn, *Anal. Commun.*, 1997, **34**, 365–369.
6 X. Zhang, S. Xu, J.-M. Lim and Y.-I. Lee, *Talanta*, 2012, **99**, 270–276.
7 L. Yea, C. Yangb, W. Lia, J. Hao, M. Suna, J. Zhang and Z. Zhang, *Food Chem.*, 2017, **217**, 389–397.
8 A. Naccarato, E. Gionfriddo, G. Sindona and A. Tagarelli, *J. Chromatogr. A*, 2014, **1338**, 164–173.
9 S. Bahrania, M. Ghaedia, M. J. Khoshnood Mansoorkhanib, A. Asfarama, A. A. Bazrafshana and M. K. Purkait, *Ultrason. Sonochem.*, 2017, **34**, 317–324.
10 D. Vuckovic, S. Risticevic and J. Pawliszyn, *Angew. Chem., Int. Ed.*, 2011, **50**, 5618–5628.
11 J. Wu and J. Pawliszyn, *J. Chromatogr. A*, 2001, **909**, 37–52.
12 J. Wu and J. Pawliszyn, *Anal. Chim. Acta*, 2004, **520**, 257–264.
13 Y. Wei, R. Hariharan and S. A. Patel, *Macromolecules*, 1990, **23**, 758–764.
14 Y. Kong, X. Shan, Y. Tao, Z. Chen and H. Xue, *J. Electrochem. Soc.*, 2013, **160**, 96–101.
15 X. Rong, F. Zhao and B. Zeng, *Talanta*, 2012, **98**, 265–271.
16 Y. Ai, J. Zhang, F. Zhao and B. Zeng, *J. Chromatogr. A*, 2015, **1407**, 52–57.
17 M. Kazemipour, M. Behzadi and R. Ahmadi, *Microchem. J.*, 2016, **128**, 258–266.
18 G. Nie, X. Han, S. Zhang, J. Xu and T. Cai, *J. Appl. Polym. Sci.*, 2007, **104**, 3129–3136.
19 C. F. Poolea and S. K. Poole, *J. Chromatogr. A*, 2010, **1217**, 2268–2286.
20 E. Aguilera-Herrador, R. Lucena, S. Cárdenas and M. Valcárcel, *Trends Anal. Chem.*, 2010, **29**, 602–616.
21 F. Q. Zhao, M. L. Wang, Y. Y. Ma and B. Z. Zeng, *J. Chromatogr. A*, 2011, **1218**, 387–391.
22 J. H. Mazurkiewicz, P. C. Innis, G. G. Wallace, D. R. Mac Farlane and M. Forsyth, *Synth. Met.*, 2003, **135**, 31–32.
23 Y. Meng, V. Pino and J. L. Anderson, *Anal. Chem.*, 2009, **81**, 7107–7112.
24 T. D. Ho, A. J. Canestraro and J. L. Anderson, *Anal. Chim. Acta*, 2011, **695**, 18–43.
25 C. Cagliero, H. Nan, C. Bicchi and J. L. Anderson, *J. Chromatogr. A*, 2016, **1459**, 17–23.
26 M. Wu, Y. Ai, B. Zeng and F. Zhao, *J. Chromatogr. A*, 2016, **1427**, 1–7.
27 J. Feng, M. Sun, L. Li, X. Wang, H. Duan and C. Luo, *Talanta*, 2014, **123**, 18–20.
28 M. A. Alawi and A. L. Azeez, *Toxin Rev.*, 2016, **35**, 69–76.
29 J. Zhao, J. Yu, Y. Xie, Z. Le, X. Hong, S. Ci, J. Chen, X. Qing, W. Xie and Z. Wen, *Sci. Rep.*, 2016, 20496.
30 M. Wu, L. Y. Wang, F. Q. Zhao and B. Z. Zeng, *RSC Adv.*, 2015, **5**, 99483–99490.
31 S. L. Zhang, Z. Du and G. K. Li, *Anal. Chem.*, 2011, **83**, 7531–7541.
32 M. H. Banitaba, S. S. H. Davarani and S. K. Movahed, *J. Chromatogr. A*, 2014, **1325**, 23–30.
33 L. Pang and J.-F. Liu, *J. Chromatogr. A*, 2012, **1230**, 8–14.
34 X. Hou, Y. Guo, X. Liang, X. Wang, L. Wang, L. Wang and X. Liu, *Talanta*, 2016, **153**, 392–400.

